Biochemical and Biophysical Research Communications 437 (2013) 173–178

Contents lists available at SciVerse ScienceDirect

Biochemical and Biophysical Research Communications

journal homepage: www.elsevier.com/locate/ybbrc

Downregulation of BTG3 in non-small cell lung cancer

Xiaobing Chen [a,b,*,1], Guoyong Chen [b,1], Xinguang Cao [a], Yudong Zhou [b], Tiejun Yang [a], Sidong Wei [b]

[a] Department of Oncology, Henan Cancer Hospital, The Affiliated Cancer Hospital of Zhengzhou University, Zhengzhou, Henan Province 450008, PR China
[b] Center of Hepatic Surgery, People's Hospital of Zhengzhou, Zhengzhou 450003, PR China

ARTICLE INFO

Article history:
Received 5 June 2013
Available online 26 June 2013

Keywords:
BTG3
Isoforms
Lung cancer

ABSTRACT

BTG3 is identified as a tumor suppressor gene in some malignancies. Btg3-deficient mice display a higher incidence of lung cancer. These results suggest that BTG3 plays an important role in lung tumorigenesis, although the underlying mechanisms are unknown. The BTG3 expression was detected using immunohistochemical staining and our results showed that the expression of BTG3 was reduced in lung cancer compared to benign lung tissues. We identified two BTG3 isoforms present in lung cancer: Full-length BTG3 and BTG3b lacking the 44 amino acids. BTG3 was predominantly expressed in benign lung tissues, whereas its expression was generally undetectable in lung cancer and cancer cell lines. Functional analysis revealed that BTG3 but not BTG3b inhibited lung cancer growth. Our results disclosed an important role of BTG3 in lung tumorigenesis.

1. Introduction

Lung cancer is a leading cause of cancer mortality worldwide; it accounts for over a million deaths annually and still has a poor prognosis [1]. Non-small cell lung cancer (NSCLC) is the predominant form of lung cancer and consists of 2 major histological subtypes: squamous cell carcinoma and adenocarcinoma [2]. It is widely accepted that NSCLC is the result of a series of molecular changes, including oncogene activation and the loss of tumor suppressor genes. Recently, the B-cell translocation gene 3 (BTG3) is identified as a tumor suppressor gene in lung cancer cells, and Btg3-deficient mice display a higher incidence of lung cancer suggesting that BTG3 plays an important role in lung tumorigenesis [3].

BTG3 is a member of the antiproliferative BTG gene family and a downstream target of p53. This family also consists of BTG1, BTG2 and BTG4 [4,5]. The members of this protein family are characterized by a N-terminal region containing two highly conserved motifs, box A and box B [6]. BTG3 is a negative regulator of the cell cycle and it has been shown that its antiproliferative action is through inhibition of transcription factor E2F1 [6,7]. In oral squamous cell carcinomas, the downregulation of the BTG3 frequently accompanied tumor development and this repression was reversed by treatment with demethylating agent (5Aza-C) suggesting that the promoter of the BTG3 gene was hypermethylated [8]. Other study shows that the BTG3 is epigenetically silenced in renal cell carcinoma and can be reactivated by genistein-induced promoter demethylation and active histone modification.

However, several issues remain unaddressed; for example, the biological consequence of the restoration of BTG3 in lung cancer cells is largely uncharacterized. Here, we delineated further the effects of the reexpression of BTG3 in lung cancer cells. Here we set out to evaluate the role of BTG3 in human lung cancer by clinical investigation and cellular experiment. We found that BTG3 was down-regulated in NSCLC compared to benign lung tissues. Our results disclosed an important role of BTG3 and alternative splicing of BTG3 in lung tumorigenesis.

2. Material and methods

2.1. Patients and tissue specimens

Tissues from patients with NSCLC were retrospectively identified from Department of Pathology, Henan Cancer Hospital. Pathology slides were analyzed according to tumor size, histologic grading and presence of nodal metastasis. All archival materials were routinely fixed in 10% neutral-buffered formalin, and embedded in paraffin. All of the tumor and macroscopically normal lung tissue samples were obtained at the time of surgery, and rapidly frozen in liquid nitrogen and stored at −80 °C until genomic DNA preparation. The macroscopically normal lung tissues were confirmed as normal by hematoxylin–eosin staining. The study was approved by the Ethics Committee at our Institution, and all patients gave their informed written consent.

* Corresponding author. Address: Department of Oncology, Henan Cancer Hospital, The Affiliated Tumor Hospital of Zhengzhou University, Henan Cancer Hospital, 127 Dong Ming Road, Jin Shui, Zhengzhou 450003, PR China.
E-mail address: chenxboncology@163.com (X. Chen).
[1] These authors contributed equally to this work.

0006-291X/$ - see front matter © 2013 Elsevier Inc. All rights reserved.
http://dx.doi.org/10.1016/j.bbrc.2013.06.062

2.2. Immunohistochemistry

Immunohistochemistry was performed by a 2-step method using primary antibody including heat-induced antigen-retrieval procedures. After dewaxed, the sections were treated with 0.3% hydrogen peroxide in methanol and 10% normal goat serum to block endogenous peroxidase and nonspecific binding, respectively. Then, they were reacted with anti-BTG3 (1:100 dilution; American Research Products, Belmont, Mass). Negative controls were treated identically but with the primary antibody omitted. Immunoreactivity was evaluated independently by 3 researchers who were blinded to patient outcome. The percentage of positive tumor cells was determined by each observer, and the average of 3 scores was calculated. We randomly selected 10 high-power fields; and counted 1000 cells in each core. When the mean of percentage of positive cells is close to 0% or 100%, the standard deviation (SD) is close to 0%, and when the mean is approximately 50% the SD is approximately 5%. Thus, the SD does not increase with the mean. The following categories were used for scoring: intensity of staining, none (0), mild (1), moderate (2), strong (3); percentage of the positive staining, <5% (0), 5–25% (1), 25–50% (2), >50% (3). Combining intensity and percentage staining resulted in the following score: 0–1, negative (−); 2–6, positive (+).

2.3. RT-PCR

To test BTG3 expression in lung cancer cells, RT-PCR was carried out. Primers used in the RT-PCR were listed in Supplementary Table S1. RNA was reverse transcribed to cDNA using SuperScript III (Invitrogen), which was then used as a template for PCR. All the experiments were performed triplicate and relative quantity was calculated after normalizing to actin expression.

2.4. Western blotting

Cells were harvested and samples (20 μg) of the cell lysate were subjected to 10% SDS–PAGE gel electrophoresis, after which the resolved proteins were transferred to nitrocellulose membranes (Amersham Biosciences). The membranes were then blocked with 5% non-fat milk and 0.1% Tween 20 in Tris-buffered saline and probed with anti-BTG3 antibody (Sigma), anti-ATG5 antibody and anti-ATG7 antibody (Cell Signaling Technology), after which the blots were visualized using enhanced chemiluminescence (Amersham, Arlington Heights, IL).

2.5. Construction of plasmids and stable cell line generation

For construction of pCMV4-flag-BTG3 and pCMV4-flag-BTG3b, the BTG3 cDNA was generated by reverse transcription PCR using BTG3 forward primer (5′-ATGAAGAATGAAATTGCTG-3′) and reverse primer (5′-TTAGTGAGGTGCTAACATGTG-3′). The sequence was confirmed by DNA sequencing, and ligated into the EcoRI and BamHI sites of pCMV-flag vector (Invitrogen). For transfection experiments, A549 cells were plated into 6-well plates 24 h before transfection. The cells were transfected with 5 μg/well of empty pCMV-flag, pCMV4-flag-BTG3 or pCMV4-flag-BTG3b using Superfect (Qiagen, Germany) according to manufacturer's instructions. For 48 h after transfection, the cells were passaged at 1:5 and cultured in medium supplemented with G418 at 500 μg/ml for 4 weeks. Clones reexpressing BTG3 (A549/BTG3) and BTG3b (A549/BTG3b) were selected for further study. As a control group, cells stably transfected with an empty vector pCMV-flag were also generated (A549/vector).

2.6. Cell cycle assay

For cell cycle assay, the cells were harvested by trypsinization, washed three times with ice-cold PBS and fixed with 70% ethanol overnight at 4 °C. The fixed cells were rehydrated in PBS and subjected to PI/RNase staining followed by fluorescence activated cell sorter scan (FACS) analysis (Becton Dickinson, Mountain View, CA, USA). The percentage of cells in each phase of the cell cycle was estimated using ELITE software.

2.7. Anchorage-independent growth

For anchorage-independent growth assay, 1×10^4 cells were plated in 0.3% low melting point agar/growth medium onto 6 cm dishs with a 0.6% agar underlay. After 3 weeks, colonies that were >1 mm in diameter were counted.

2.8. Tumorigenicity assay

Six-week-old male nude mice were housed under standard conditions. The cell were trypsinized, washed with PBS, and suspended in RPMI 1640 without serum. A total of 2×10^6 cells were subcutaneously injected into the flanks of the nude mice. Tumor growth was measured every 2 days, and tumor volume was estimated as length $\times$ width^2 $\times$ 0.52.

2.9. Electron microscopy

Treated cells were washed and fixed for 30 min in 2.5% glutaraldehyde. The samples were treated with 1.5% osmium tetroxide, dehydrated with acetone and embedded in Durcupan resin. Thin sections were poststained with lead citrate and examined in the TECNAI 10 electron microscope (Philips, Holland) at 60 kV.

2.10. Statistical analysis

All data are given as the mean ± standard deviation (SD). Statistical analyses were conducted using two-tailed paired student's *t*-tests. $P < 0.05$ was considered statistically significant.

3. Results

3.1. Expression profile of BTG3 in NSCLC

We first detected the expression of BTG3 protein in a TMA of primary NSCLC and adjacent normal lung tissue specimens using immunohistochemical staining with a specific anti-BTG3 antibody. Representative examples of BTG3 protein expression in NSCLC and normal lung samples are shown in Fig. 1. We found a significant difference in BTG3 expression between NSCLC and normal lung tissue specimens (Fig. S1). Overall, expression of BTG3 was absent in 50 of 60 in lung cancer samples (83%), whereas the expression of BTG3 in all normal lung tissues was detectable.

To further validate these results, semiquantitative reverse transcription-PCR (RT-PCR) analysis from 10 patients with NSCLC was conducted by using BTG3-specific primers. Notably, two PCR products were readily detected after amplification. We found that BTG3 mRNA is expressed as two variants: full-length and an alternatively spliced version lacking 144 bps, which was confirmed by DNA sequencing (Fig. S2). PCR analysis revealed that BTG3 not BTG3b was the predominant isoform expressed in nonmalignant lung tissues, whereas BTG3b expression did not differ significantly in NSCLC and normal lung tissue (Fig. 2A). Furthermore, by western blot, we revealed a significant downregulation of BTG3 in the tumor specimens compared with nonmalignant lung tissues,

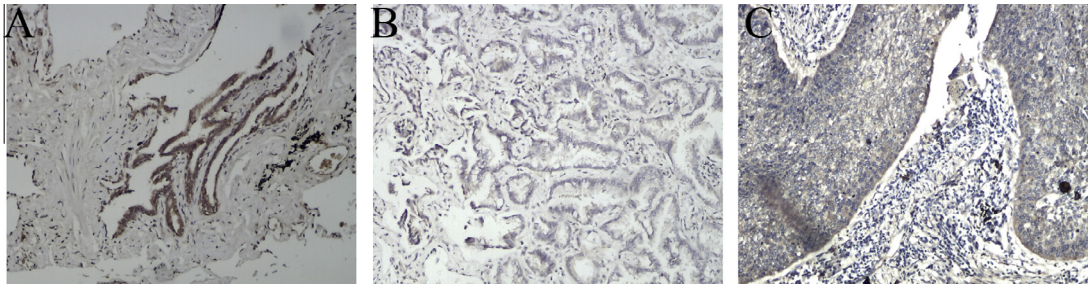

Fig. 1. Immunohistochemical staining for BTG3 with anti-BTG3 in the cancerous and normal tissues. The nuclei were countered stained with hematoxylin. (A) Bronchial epithelial cells showed strong BTG3 staining. Weaker BTG3 expression in (B) Adenocarcinoma and (C) squamous cell carcinoma (magnification, 200×).

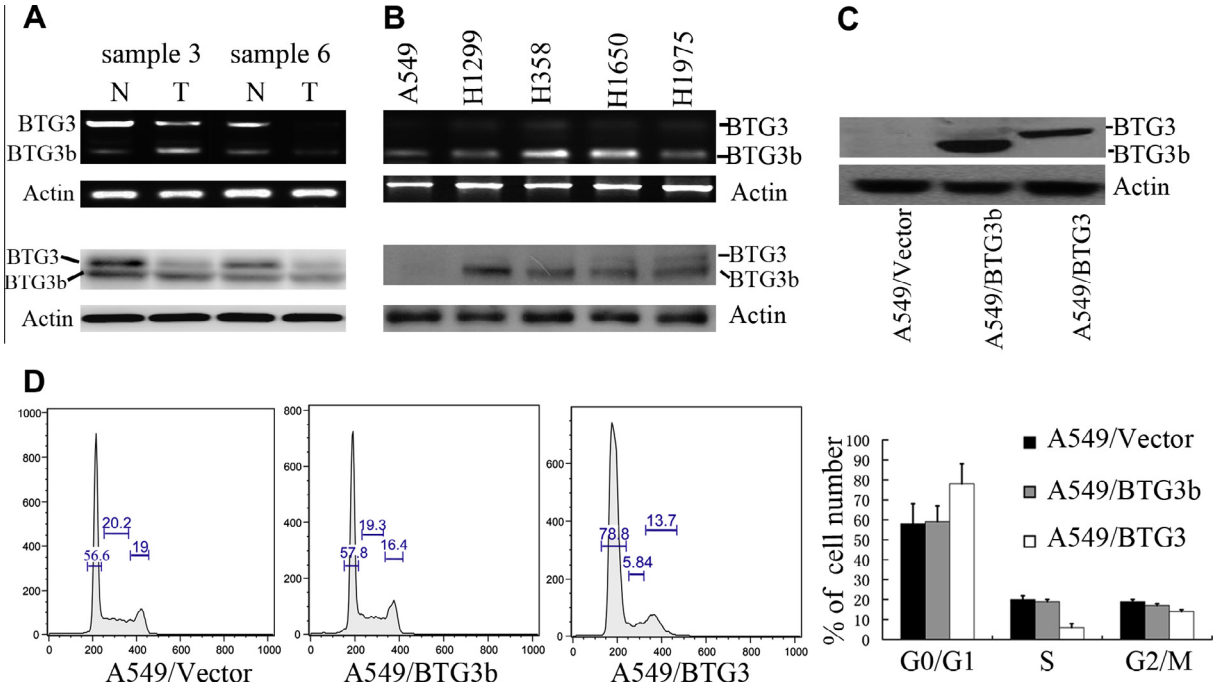

Fig. 2. (A) The mRNA and protein levels of BTG3 in primary lung cancer and adjacent normal lung tissue. (B) The mRNA and protein levels of BTG3 in lung cancer cell lines. (C) Forced expression of BTG3 and BTG3b in A549/BTG3 and A549/BTG3b was verified by Western blot. (D) Exogenous expression of BTG3 induces cell cycle G1 arrest in lung cancer cells. Cell cycle progression of A549/BTG3, A549/BTG3b and A549/vector cells was determined by FACS analysis. Data are representative of three independent experiments.

whereas BTG3b expression did not differ significantly in NSCLC and normal lung tissue (Fig. 2B).

3.2. Downregulation of BTG3 is associated with lung cancer differentiation and metastasis

To characterize the correlation between downregulation of BTG3 and clinical features of lung cancer, several clinicopathological characteristics including age, gender, cell differentiation, tumor size, lymph node (LN) metastases and smoking status were compared between patients with or without expression of BTG3 (Table 1). This result indicated that expression of BTG3 was not associated with histology ($P = 0.322$), tumor size ($P = 0.098$), smoking status ($P = 0.207$), patient's age and gender (data not shown). However, expression of BTG3 was significantly correlated with LN metastasis ($P = 0.013$) and poor differentiation ($P = 0.002$). Because BTG3 isoform-specific antibodies are currently unavailable, our immunostaining results did not reveal the isoform identities of BTG3 proteins.

3.3. Exogenous expression BTG3 alters lung cancer cell cycle

To assess whether isoforms of BTG3 affect the biological behavior of lung cancer cells, we established BTG3 and BTG3b expression plasmid. Then we established A549/BTG3 and A549/BTG3b which stably express BTG3 and BTG3b, respectively. The expression of BTG3 and BTG3b in A549/BTG3 and A549/BTG3b cells was confirmed by Western analysis (Fig. 2C). Cell growth was analyzed using MTT assays which were performed in triplicate in 96 well plates. Compared with the A549/BTG3b and A549/vector cells, the proliferation of A549/BTG3 cells was inhibited (data not shown).

To further understand the mechanisms by which cell proliferation is affected, flow cytometry was performed to analyze the cell cycle phase distribution of these cells. The cell cycle progression of A549/BTG3 cells was stalled at the G1 phase with a significant decrease in S and G2/M phases compared with A549/BTG3b and A549/vector cells (Fig. 2D). To further validate these results, we also established H358/BTG3 and H358/BTG3b which stably express BTG3 and BTG3b, respectively. Similarly, we found that the cell cy-

Table 1
Clinical characteristics of NSCLC patients according to expression status of BTG3.

Group	BTG3 expression		*P* value
	–	+	
Cancer tissues	50	10	
Histology			
ADC	23	6	0.322
SCC	27	4	
Differentiation			
Well	2	4	0.002
Moderate	27	4	
Poor	21	2	
LN metastasis			
Yes	32	2	0.013
No	18	8	
Size (cm)			
<3	26	8	0.098
⩾3	24	2	
Smoking status			
Yes	30	4	0.207
No	20	6	

ADC, adenocarcinoma; SCC, squamous cell carcinoma.

cle progression of H358/BTG3 cells was stalled at the G1 phase with a significant decrease in S and G2/M phases compared with H358/BTG3b and H358/vector cells (Fig. S3).

3.4. Reexpression of BTG3 inhibits anchorage-independent growth and tumor growth in mice

We further showed the growth inhibitory features of BTG3 reintroduction in colony formation assay and nude models. The effect BTG3 on anchorage-independent growth in a soft agar colony formation assay was assessed in A549 and H358 cells. These cells were seeded and incubated in soft agar for 8 weeks. Each experiment was done in triplicate with three independent clones. A549/vector and H358/vector showed robust colony growth, whereas colony growth was greatly reduced when BTG3 but not BTG3b was reexpressed (Figs. 3A and S4).

We examined the ability of A549/BTG3 and A549/BTG3b cells to form tumors compared to A549/vector. All mice injected with A549/BTG3, A549/BTG3b and A549/vector cells developed palpable tumors. Tumors derived from A549/BTG3b and A549/vector cells were 2–2.5 times larger than that derived from A549/BTG3 cells ($P < 0.001$) (Fig. 3B). There is no significant difference between A549/BTG3b and A549/vector cells.

3.5. Reexpression of BTG3 inhibits autophagy in lung cancer cells

BTG3 depletion in normal human fibroblasts led to cellular senescence [9]. The expression of senescence-associated genes, such as MMP-1 and PAI-1, was elevated in normal human fibroblast IMR90 cells when the BTG3 was silenced [9]. Here, we investigate whether BTG3 is implicated in autophagy, which is closely associated with cellular senescence. We found that the mRNA levels of MMP-2 and PAI-1 are decreased in A549/BTG3 cells compared to A549/BTG3b and A549/vector cells (Fig. S5). Ultrastructural analysis by electron microscopy confirmed that numerous large autophagic vacuoles with typical double-layer membrane containing organelle remnants presented in A549/BTG3b and A549/vector cells rather than A549/BTG3 when these cells were treated with 4 nM paclitaxel (Fig. 4A). To molecularly confirm the induction of autophagy, we measured the expression of autophagy-related proteins. Reexpression of BTG3 inhibits the

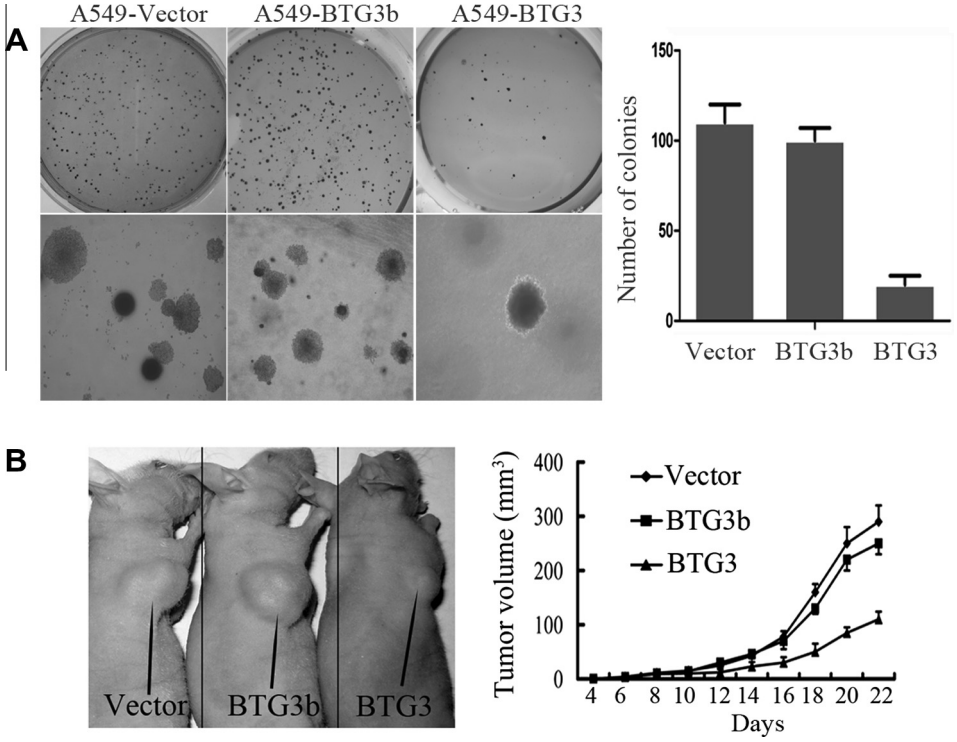

Fig. 3. Forced expression of BTG3 inhibits anchorage-independent growth and tumor growth in mice. (A) Examples of colony assay after 4-week selection. Left bottom, detailed images from the top panels (magnification, 400×). Cells were stained with Giemsa, colonies were counted. Graph represents means of three independent experiments ± standard deviations. (B) Effect of BTG3 on the growth of lung cancer cells in nude mice. Shown are tumors in nude mice 1 month after injection of 2×10^6 A549/BTG3, A549/BTG3b and A549/vector cells. The tumor volume of A549/BTG3, A549/BTG3b and A549/vector cells in nude mice was indicated as mean tumor volume ± SD (mm^3). Tumor mean volume of A549/BTG3 mice was significantly smaller than the A549/BTG3b and A549/vector nude mice group.

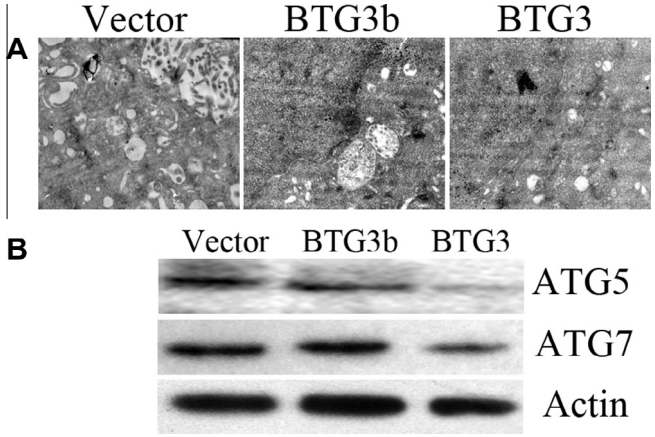

Fig. 4. Reexpression of BTG3 inhibits autophagy in lung cancer cells. (A) Electron microscopy confirmed that numerous large autophagic vacuoles with typical double-layer membrane containing organelle remnants presented in A549/BTG3b and A549/vector cells rather than A549/BTG3 when these cells were treated with 4 nM paclitaxel. (B) Immunoblotting for ATG5 and ATG7 using lysates from A549/BTG3, A549/BTG3b and A549/vector. Reexpression of BTG3 inhibits the increase of ATG5 and ATG7 in A549/BTG3 cells not A549/BTG3b or A549/vector cells after treatment of paclitaxel.

increase of ATG5 and ATG7 in A549/BTG3 and H358/BTG3 cells not A549/BTG3b, A549/vector, H358/BTG3b or H358/vector cells after treatment of paclitaxel (Figs. 4B and S6).

4. Discussion

Down-regulation of BTG3 through promoter methylation has been observed in renal, breast, and prostate cancers [10–12]. These results suggest that BTG3 plays an important role in tumor suppression, although the underlying mechanisms are unknown. BTG3-knockout mice display a higher incidence of lung tumors, which correlates with reduced expression in clinical specimens from lung cancer [3]. However, other studies failed to observe the reduction of BTG3 expression in lung cancer, indicating that the status of BTG3 expression inlung cancer needs further investigation [9].

In the present study, we first determined the expression level of BTG3 in primary human NSCLC and adjacent non-cancer tissues by immunohistochemistry and RT-PCR. When compared to adjacent non-cancer tissues, BTG3 was found to be significantly downregulated in NSCLC. We also found that expression of BTG3 was significantly correlated with LN metastasis ($P < 0.001$) and poor differentiation in lung cancer.

Using BTG3-specific primers, we found that BTG3 mRNA is expressed as two variants: full-length and an alternatively spliced version lacking 144 bps, which was confirmed by DNA sequencing. We revealed a significant downregulation of BTG3 in the tumor specimens compared with nonmalignant lung tissues, whereas BTG3b expression did not differ significantly in lung tumors and normal lung tissue. Because BTG3 isoform-specific antibodies are currently unavailable, our immunostaining results did not reveal the isoform identities of BTG3 proteins.

Overexpression of the candidate tumor suppressor BTG3 suppresses cell growth; conversely, its deficiency enhances cell proliferation in cancer cells. However, it was reported that restoration of BTG3 in lung cancer cells did not affect either the colony formation rate or cell proliferation rate [9]. Apparently, much remains to be learned regarding the regulation of cell proliferation by BTG3 reduction of BTG3 expression in lung cancer. To assess whether isoforms of BTG3 affect the biological behavior of lung cancer cells, we established BTG3 and BTG3b expression plasmid. Then we established A549/BTG3, A549/BTG3b, H358/BTG3 and H358/BTG3b which stably express BTG3 and BTG3b, respectively.

Compared with the A549/BTG3b, H358/BTG3b, H358/vector and A549/vector cells, the proliferation of A549/BTG3 and H358/BTG3 cells was inhibited. To further understand the mechanisms by which cell proliferation is affected, flow cytometry was performed to analyze the cell cycle phase distribution of these cells. The cell cycle progression of A549/BTG3 and H358/BTG3 cells was stalled at the G1 phase with a significant decrease in S and G2/M phases compared with A549/BTG3b, H358/BTG3b, H358/vector and A549/vector cells. BTG3 associates with and inhibits the transcription factor E2F1 and is involved in the regulation of S phase entry and maintenance of G2 arrest. However, we did not observe the similar results in A549 lung cancer cells. We also found that reexpression of BTG3 inhibits anchorage-independent growth and tumor growth in mice. This was in contrast to other studies that failed to detect the alteration of the colony formation rate or cell proliferation rate by restoration of BTG3 in lung cancer cells. The functional relevance of these findings needs further investigation [9]. Taken together, these results suggest that enforced expression of BTG3 plays an important role in lung cancer cell biology, whereas BTG3b does not have any such effects. Furthermore, the protein–protein interaction between BTG3 and BTG3b was not observed by coimmunoprecipitation. These results suggest that much remains to be done to figure out the exact role of BTG3b in lung cancer cell biology.

Autophagy is a membrane-trafficking process that delivers cytoplasmic constituents to lysosomes for degradation [13]. Although a role in cancer is unquestionable, there are contradictory reports that autophagy can be both oncogenic and tumor suppressive, perhaps indicating that autophagy has different roles at different stages of tumor development [14]. Autophagy is reportedly closely related with cellular senescence and inhibition of autophagy delays cellular senescence in mitotic human diploid cells [15,16]. BTG3 depletion in normal human fibroblasts led to cellular senescence. The expression of senescence-associated genes, such as MMP-1 and PAI-1, was elevated in normal human fibroblast IMR90 cells when the BTG3 was silenced. We found that the mRNA levels of MMP-2 and PAI-1 are decreased in A549/BTG3 cells compared to A549/BTG3b and A549/vector cells. Ultrastructural analysis by electron microscopy confirmed that numerous large autophagic vacuoles with typical double-layer membrane containing organelle remnants presented in A549/BTG3b and A549/vector cells rather than A549/BTG3 when these cells were treated with 4nM paclitaxel. The protein levels of ATG5 and ATG7, the most important components for the formation of autophagosome, were decreased when BTG3 expression was restored.

In this study, we found that the expression of BTG3 was reduced in lung cancer compared to benign lung tissues. Our results disclosed an important role of BTG3 in lung tumorigenesis.

Acknowledgments

The authors greatly appreciate the technical assistance of Mrs. Shidan Chen. The authors thank Mrs. Zhao Lin for their assistance. This research was supported by National Natural Science Foundation of China (Grant No.81172240).

Appendix A. Supplementary data

Supplementary data associated with this article can be found, in the online version, at http://dx.doi.org/10.1016/j.bbrc.2013.06.062.

References

[1] T. Koga, M. Takeshita, T. Yano, Y. Maehara, K. Sueishi, CHFR hypermethylation and EGFR mutation are mutually exclusive and exhibit contrastive clinical backgrounds and outcomes in non-small cell lung cancer, Int. J. Cancer 128 (2011) 1009–1017.

[2] K.M. Hong, S.H. Yang, S.R. Chowdhuri, A. Player, M. Hames, J. Fukuoka, D. Meerzaman, T. Dracheva, Z. Sun, P. Yang, J. Jen, Inactivation of LLC1 gene in nonsmall cell lung cancer, Int. J. Cancer 120 (2007) 2353–2358.

[3] M. Yoneda, T. Suzuki, T. Nakamura, R. Ajima, Y. Yoshida, S. Kakuta, S. Katsuko, Y. Iwakura, M. Shibutani, K. Mitsumori, J. Yokota, T. Yamamoto, Deficiency of antiproliferative family protein Ana correlates with development of lung adenocarcinoma, Cancer Sci. 100 (2009) 225–232.

[4] U. Cortes, C. Moyret-Lalle, N. Falette, C. Duriez, F.E. Ghissassi, C. Barnas, A.P. Morel, P. Hainaut, J.P. Magaud, A. Puisieux, BTG gene expression in the p53-dependent and -independent cellular response to DNA damage, Mol. Carcinog. 27 (2000) 57–64.

[5] Y.C. Cheng, T.Y. Lin, S.Y. Shieh, Candidate tumor suppressor BTG3 maintains genomic stability by promoting Lys63-linked ubiquitination and activation of the checkpoint kinase CHK1, Proc. Natl. Acad. Sci. USA 110 (2013) 5993–5998.

[6] S. Majid, A.A. Dar, A.E. Ahmad, H. Hirata, K. Kawakami, V. Shahryari, S. Saini, Y. Tanaka, A.V. Dahiya, G. Khatri, R. Dahiya, BTG3 tumor suppressor gene promoter demethylation, histone modification and cell cycle arrest by genistein in renal cancer, Carcinogenesis 30 (2009) 662–670.

[7] Y.H. Ou, P.H. Chung, F.F. Hsu, T.P. Sun, W.Y. Chang, S.Y. Shieh, The candidate tumor suppressor BTG3 is a transcriptional target of p53 that inhibits E2F1, EMBO J. 26 (2007) 3968–3980.

[8] N. Yamamoto, K. Uzawa, T. Yakushiji, T. Shibahara, H. Noma, H. Tanzawa, Analysis of the ANA gene as a candidate for the chromosome 21q oral cancer susceptibility locus, Br. J. Cancer 84 (2001) 754–759.

[9] T.Y. Lin, Y.C. Cheng, H.C. Yang, W.C. Lin, C.C. Wang, P.L. Lai, S.Y. Shieh, Loss of the candidate tumor suppressor BTG3 triggers acute cellular senescence via the ERK-JMJD3-p16(INK4a) signaling axis, Oncogene 31 (2011) 3287–3297.

[10] M. Putnik, C. Zhao, J.A. Gustafsson, K. Dahlman-Wright, Global identification of genes regulated by estrogen signaling and demethylation in MCF-7 breast cancer cells, Biochem. Biophys. Res. Commun. 426 (2012) 26–32.

[11] S. Majid, A.A. Dar, V. Shahryari, H. Hirata, A. Ahmad, S. Saini, Y. Tanaka, A.V. Dahiya, R. Dahiya, Genistein reverses hypermethylation and induces active histone modifications in tumor suppressor gene B-Cell translocation gene 3 in prostate cancer, Cancer 116 (2010) 66–76.

[12] J. Yu, Y. Zhang, Z. Qi, D. Kurtycz, G. Vacano, D. Patterson, Methylation-mediated downregulation of the B-cell translocation gene 3 (BTG3) in breast cancer cells, Gene Expr. 14 (2008) 173–182.

[13] W. Han, H. Pan, Y. Chen, J. Sun, Y. Wang, J. Li, W. Ge, L. Feng, X. Lin, X. Wang, X. Wang, H. Jin, EGFR tyrosine kinase inhibitors activate autophagy as a cytoprotective response in human lung cancer cells, PLoS ONE 6 (2011) e18691.

[14] X. Sui, L. Jin, X. Huang, S. Geng, C. He, X. Hu, P53 signaling and autophagy in cancer: a revolutionary strategy could be developed for cancer treatment, Autophagy 7 (2011) 565–571.

[15] Y.Y. Cho, D.J. Kim, H.S. Lee, C.H. Jeong, E.J. Cho, M.O. Kim, S. Byun, K.Y. Lee, K. Yao, A. Carper, A. Langfald, A.M. Bode, Z. Dong, Autophagy and cellular senescence mediated by Sox2 suppress malignancy of cancer cells, PLoS ONE 8 (2013) e57172.

[16] A.R. Young, M. Narita, M. Ferreira, K. Kirschner, M. Sadaie, J.F. Darot, S. Tavare, S. Arakawa, S. Shimizu, F.M. Watt, M. Narita, Autophagy mediates the mitotic senescence transition, Genes Dev. 23 (2009) 798–803.